

Biosensing platform combining label-free and labelled analysis using Bloch surface waves

Norbert Danz^{a,*}, Alberto Sinibaldi^b, Peter Munzert^a, Aleksei Anopchenko^b, Erik Förster^a, Stefan Schmieder^c, Rona Chandrawati^d, Riccardo Rizzo^{a,b}, Rene Heller^e, Frank Sonntag^c, Alessandro Mascioletti^f, Subinoy Rana^d, Thomas Schubert^e, Molly M. Stevens^d and Francesco Michelotti^b

^a Fraunhofer Institute for Applied Optics and Precision Engineering IOF, 07745 Jena, Germany;

^b Basic and Applied Science for Engineering Department (SBAI), SAPIENZA Università di Roma, 00161 Roma, Italy;

^c Fraunhofer Institute for Material and Beam Technology IWS, 01277 Dresden, Germany;

^d Department of Materials, Imperial College London, London SW7 2AZ, UK

^e Radeberger Präzisions- Formen- und Werkzeugbau, Großröhrsdorf, Germany

^f Labor S.r.l., Tecnopolo Tiburtino, 00131 Roma, Italy

ABSTRACT

Bloch surface waves (BSW) propagating at the boundary of truncated photonic crystals (1D-PC) have emerged as an attractive approach for label-free sensing in plasmon-like sensor configurations. Due to the very low losses in such dielectric thin film stacks, BSW feature very low angular resonance widths compared to the surface plasmon resonance (SPR) case. Besides label-free operation, the large field enhancement and the absence of quenching allow utilizing BSW coupled fluorescence detection to additionally sense the presence of fluorescent labels. This approach can be adapted to the case of angularly resolved resonance detection, thus giving rise to a combined label-free / labelled biosensor platform. It features a parallel analysis of multiple spots arranged as a one-dimensional array inside a microfluidic channel of a disposable chip. Application of such a combined biosensing approach to the detection of the Angiopoietin-2 cancer biomarker in buffer solutions is reported.

Keywords: optical biosensors, Bloch surface waves, fluorescence and luminescence, photonic crystal, label-free optical sensors, optical multilayer systems

1. INTRODUCTION

Sensors utilizing surface plasmon resonance (SPR) are established as the method of choice in label-free optical biosensing^{1,2}, and a variety of optical approaches including imaging, angularly and spectrally resolved resonance tracking are applied to read the transducers information. Recently, Bloch surface waves (BSW) propagating at the boundary of truncated one dimensional photonic crystals^{3,4} (1D-PC) have been suggested to be applied in SPR-like sensing configurations^{5,6} comprising angularly resolved detection modes.

BSW feature very low resonance widths compared to that of SPR due to the very low losses in the state-of-the-art dielectric thin film stacks⁷. Furthermore, BSW sensors offer the possibility to optimize the resonance, i.e., to tune its position and width as the most important parameters. Utilizing appropriate merit functions⁸ allows optimizing the 1D-PC stack for optimum label-free operation⁹. However, label-free sensing might still suffer from less-than-ideal suppression or referencing of unspecific effects and yield a non-adequate limit of detection in the small concentration range of the analytes. Therefore, a complementary detection system relying on the detection of fluorescent labels could potentially increase the system's variability and decrease the limit of detection, which is crucial in biosensing applications. The large field enhancement at the 1D-PC surface and the absence of quenching favor utilizing BSW coupled fluorescence emission^{10,11}. In such a configuration, the surface wave is exploited in a twofold manner: First, the resonance position is

* norbert.danz@iof.fraunhofer.de

tracked as a label-free signal. Second, surface wave coupled emission yields a specific fluorescence detection whenever a labelling step is performed.

We report on the development and initial results of such combined biosensing platform utilizing disposable sensor chips. Based on our previous work on angularly resolved SPR analysis^{7,12}, a new optical system has been designed and fabricated. The new system features the combination of SPR-like angularly resolved resonance and the detection of fluorescent labels. All analysis can be performed in a parallel manner for multiple spots that are arranged as a one-dimensional array inside a microfluidic channel. In order to enable for later on disposable use, injection molded polymer substrates have been prepared and coated with low loss 1D-PC.

The transducing thin film stack is explained in detail in section 2, along with its simulated properties with regard to label-free sensing and fluorescence emission pattern modification. Section 3 introduces the basic optical system concept. Proof-of-principle operation is demonstrated by the detection of Angiopoietin-2 (Ang2) in buffer solutions. Ang2 plays an important role in embryonic and postnatal angiogenesis, thus making it a clinical marker for angiogenesis and early stage cancer development in adults^{13,14}. The corresponding chip preparation and assay approach are described in section 4 prior to illustrating the experimental results in section 5. These results demonstrate the validity of the approach and will be discussed in section 6.

2. CHIPS AND DIELECTRIC THIN FILM STACK

Injection molded polymer chips made of TOPAS[®] were purposely developed and manufactured by KDS Radeberg (Figure 1). These comprise a prism shaped cross section in order to excite the surface wave in Kretschmann configuration. Additionally, two-component flow cell has been molded. It consists of a hard polymer cover that can be clicked by hand onto the chip. Inside this cover an elastomer defines a straight micro channel of 800 μm x 100 μm cross section as well as perpendicularly aligned fluid connectors.



Figure 1. Photograph of an injection molded chip coated with dielectric thin film stack and a flow cell, the latter being prepared by two-component molding.

The dielectric stacks were fabricated by plasma ion assisted evaporation under high vacuum conditions using an APS904 coating system (Leybold Optics). After initial cleaning the substrates were preconditioned by plasma etching with the APS plasma source and low ion energies for 60 s. SiO_2 (silica), Ta_2O_5 (tantala) and TiO_2 (titania) had been chosen as dielectric materials. In order to achieve low internal stress levels and absorption losses, a medium level argon ion assistance with ion energies of about 120 eV was applied¹⁵. Material evaporation was performed by an electron beam gun to obtain deposition rates of 0.5 nm/s, 0.4 nm/s, and 0.25 nm/s for SiO_2 , Ta_2O_5 , and TiO_2 layers, respectively. Single layer thicknesses were tracked by a quartz crystal monitor during deposition.

The complex refractive indices of the materials were determined either by reflection/transmission spectroscopy on single supported thin films or by ellipsometry on test multilayers sustaining BSW to be $n_{\text{SiO}_2} = 1.474 + i 5 \times 10^{-6}$, $n_{\text{Ta}_2\text{O}_5} = 2.160 + i 5 \times 10^{-5}$, and $n_{\text{TiO}_2} = 2.28 + i 1.8 \times 10^{-3}$ at the label-free wavelength of operation $\lambda_0=670$ nm. Using such values enables one to optimize the stacks according to the considerations published elsewhere⁹. The final structure of the stack is shown in Figure 2 and has been previously applied for an ellipsometric sensing approach¹⁶. In this stack, a 20 nm thin TiO_2

layer is combined with a periodic $\text{SiO}_2 / \text{Ta}_2\text{O}_5$ stack comprising 275 nm and 120 nm thicknesses, respectively. In order to work with silane based functionalization protocols, the stack is covered with a 20 nm thin SiO_2 layer.

Figure 2(b) illustrates the dispersion of the resonance in the wavelength-angle-plane. Two surface modes exhibiting different polarization are apparent. The TE resonance has been optimized for label-free sensing, but the stack design supports a rather wide and shallow TM mode at lower angles (wavelengths). For the present study only the TE polarized mode is utilized for label-free operation, although both polarizations might be exploited e.g. in ellipsometric approaches⁸.

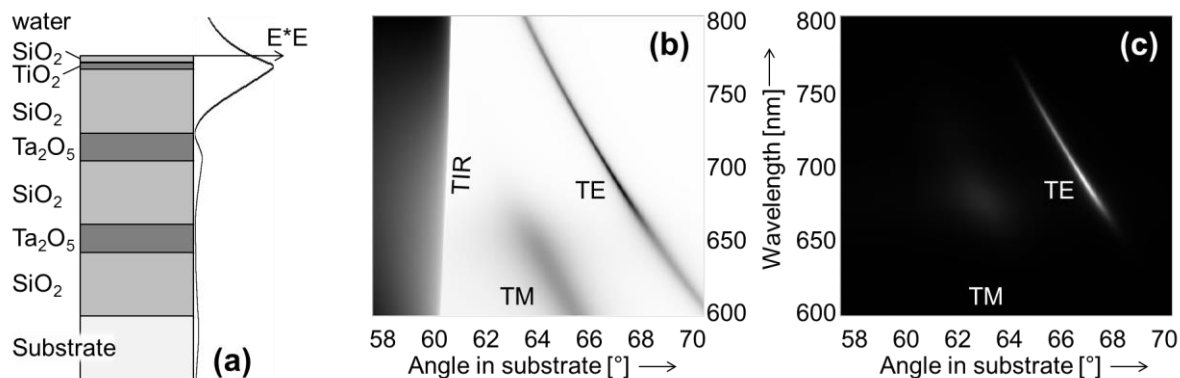


Figure 2. (a) Sketch of the dielectric thin film stack with TE energy density distribution of the resonance at 670 nm wavelength. (b) Grey scale plot of angularly and spectrally resolved reflectivity of the stack when illuminated from the substrate. (c) Emission pattern of DyLight650 dye molecules located on top of the thin film stack and plotted in grey scale representation. The labels “TE” and “TM” indicate the polarization of the resonances and “TIR” the dispersion of the total internal reflection edge.

The fluorescence emitted by randomly oriented dye labels located on top of such stack is simulated rigorously by means of a transfer-matrix algorithm¹⁷ frequently applied for the modelling of Organic LED¹⁸. In Figure 2(c) we show the results when the emission spectrum of the DyLight650 dye (Abcam, UK) is assumed¹⁹. It is observed that the fluorescence energy is coupled preferentially into the surface modes, giving rise to a sharp resonance enhancement¹⁰. The dispersion of such spontaneous emission is identical to the dispersion of the resonance. Thus, each wavelength is emitted at a slightly different angle as defined by the thin film stack’s dispersion. Combining this effect with the optical concept of angularly resolved emission yields an expected fluorescence angular distribution as shown in Figure 3. Each polarized component of the emission (TE or TM) is detected as a separate peak, comprising an angularly dependent wavelength as given by the dispersion of the surface wave in Figure 2(c). It should be noted that the angular dispersion as well as the angular separation of polarized emission is due to stack design and might be altered by adapting the thin film system.

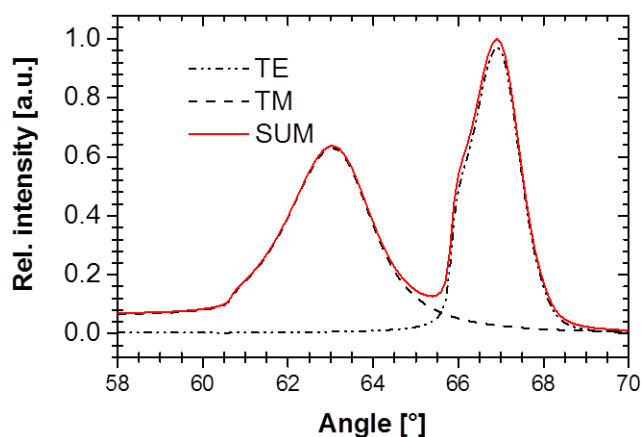


Figure 3. Angular spectrum of fluorescence simulated for the emission pattern in Figure 2(c) when taking into account the spectral transmittance of filters inserted in the fluorescence collection optics.

3. OPTICAL ANALYSIS

The optical system approach is derived from a system previously developed for parallel SPR analysis on polymer chips¹² the performance of which has been demonstrated recently^{20,21}. A simplified overview of the optical system modified for BSW based analysis is presented in Figure 4. A collimated light beam B is focused by means of a cylindrical lens C1 into the chip described above (Figure 1). The prismatic shape is required to illuminate the sensor surface above the critical angle for total internal reflection (TIR). As indicated in Figure 4 the surface is coated with the dielectric thin film stack described in section 2. This approach creates an illuminated line along the direction x on the surface. Several measurement areas (“spots”) can be arranged in a row along this illuminated line. Parallel readout of these spots is achieved by using a cylindrical detection optical system that consists of objective (C2) and tube lens (C3) systems in order to image the direction x onto one coordinate of a CCD detector. The design of the optical detection system ensures that the same angular range is observed for all spots along the illuminated region on the sensor surface.

In contrast to previous work⁷ a laser diode (670 nm wavelength) is utilized for label-free analysis to achieve proper resolution of the narrow angular BSW resonances. Furthermore, the detection optical system features an extended CCD detector (Apogee Ascent equipped with Sony ICX814 CCD chip) to obtain 3388 (angular axes) and 2712 (position axes) pixels readout. The lateral field of view (coordinate x in Figure 4) is approximately 6 mm and 8 pixels binning is applied because of the limited spatial resolution of lateral imaging. The angular field of view is determined by cylindrical Fourier lens F to be approximately 2.9°. Full discretization of the CCD chip (no binning) is exploited in order to achieve proper sampling of the resonance. For label-free detection the region of interest (ROI) is reduced to approximately 1’200 pixels around the resonance in order to decrease the time needed for CCD read out and data transmission.

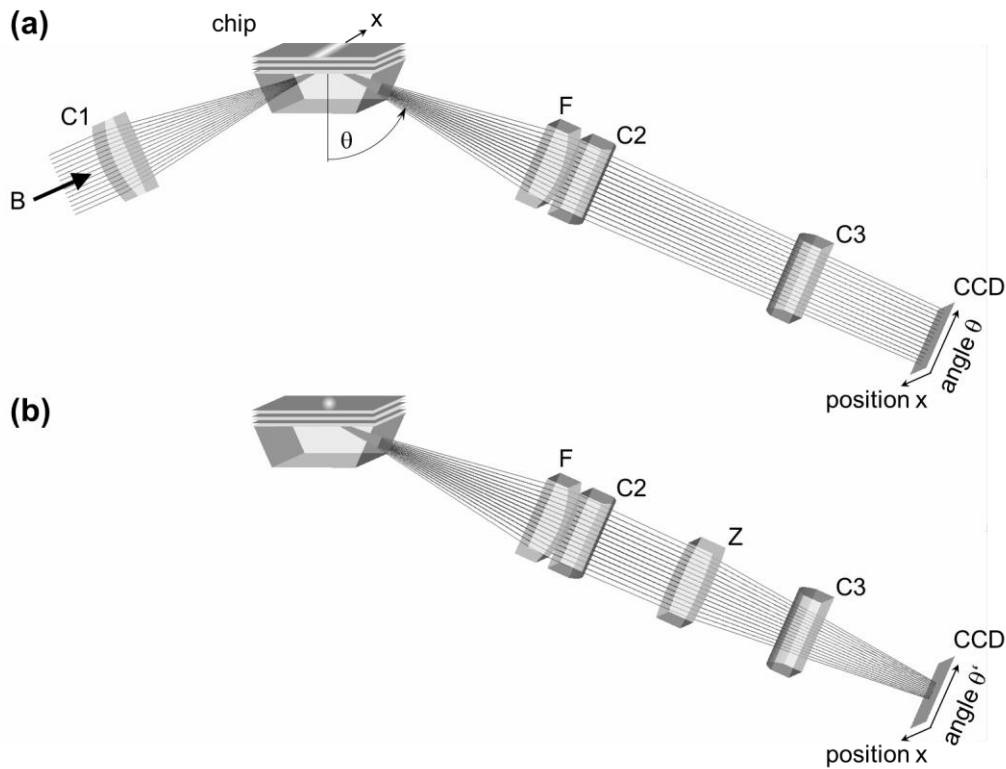


Figure 4. Simplified view of the optical system in label-free (a) and fluorescence (b) modes. In the label-free mode (a) a collimated beam (B) is focused by means of a cylindrical lens (C1) into the chip to create an illuminated line. Cylindrical objective (C2) and tube lens systems (C3) image the lateral coordinate onto one axes of the CCD detector. A Fourier lens F images the angular spectrum of light reflected at the sensor surface onto the CCD detector. An additional cylindrical lens (Z) is introduced for fluorescence detection (b) to increase the angular detection range.

Fluorescence detection follows the approach described recently¹¹ and is based on 635 nm illumination. Spatial imaging and binning are identical to the label-free case. However, Figure 3 illustrates that the angular range of 2.9° is too small to detect both emission polarizations. Therefore, an additional cylindrical lens Z in Figure 4(b) is introduced into the light path in order to increase the angular field of view. The limited angular resolution associated with this approach is acceptable, and consequently angular binning of 8 pixels is utilized in fluorescence detection mode.

Filter elements for selecting a certain polarization and/or spectral range are arranged in-between the cylindrical objective (C2) and tube lens (C3) systems. The spectral fluorescence emission filter (Chroma 685/70) is fixed in the detection optics because the label-free operation wavelength of 670 nm is well within the fluorescence emission band and transmits such element.

4. CHEMICALS AND CHIP PREPARATION

Chip preparation

In order to obtain a clean silica surface of the biochips, the surfaces were exposed to a piranha solution (3:1 mixture of concentrated sulfuric acid and 30% hydrogen peroxide solution) for 10 minutes. Subsequently, the substrates were carefully rinsed with de-ionized (DI) water and dried under a stream of nitrogen gas. The cleaned biochips were then immersed into a 2% (v/v) solution of APTES ((3-Aminopropyl)triethoxysilane from Sigma-Aldrich) in ethanol/water (95:5 v/v) mixture at room temperature (RT) for 1 h. Afterwards the chips were removed from the solution, sonicated (~30 s), rinsed with ethanol, and dried on a hot plate at 80°C for 1 h.

Protein immobilization starts with the coupling of the linker with 1% (v/v) glutaraldehyde (Sigma-Aldrich) solution in 100 mM sodium bicarbonate buffer (pH 8.5) in the presence of 0.1 mM NaCNBH₃ (sodium cyanoborohydride, Sigma-Aldrich) for 1 h at room temperature. A further sonication in DI water was performed prior to thoroughly rinsing the biochips with DI water. A 0.5 mg/ml solution of Protein G (Thermo Scientific) in sodium bicarbonate buffer was brought in contact with one part of the sensing area that will be referred to as “measurement spot”. A second part of the sensor surface was incubated with 10 mg/mL of bovine serum albumin (BSA, from Sigma-Aldrich) to serve as the “reference”. Protein coupling was stopped after 1 h interaction time at room temperature by washing away residual solution. Finally, the full surface was immersed in 10 mg/ml of BSA overnight at 4°C in order to block remaining reactive sites. In result, capture antibodies can be coupled later on with Fc fragment to the protein G (“measurement”) surface in order to maintain their functional Fab sites for specific detection.

Immediately before use the surface of the biochips was treated with a regeneration solution made of 20 mM glycine (Sigma-Aldrich) and HCl with a pH of 2.5 for 10 min at RT. This step improves the recovery of surface reactivity after the blocking step in BSA, because any adlayers should be removed from the covalently linked protein layers. All other reagents such as ethanol (99.8%), sulfuric acid (95%), 30% hydrogen peroxide solution and phosphate buffer saline (PBS, pH 7.4) were obtained from Sigma-Aldrich and were used as it is.

Cancer Biomarker Assay

Ang2, a factor playing an important role in embryonic and postnatal angiogenesis, has been selected for demonstration purposes. Therefore, a specific capture antibody was immobilized via its Fc fragment onto the Protein G-coated “measurement” surface. Note, that all the following steps were performed in the fluidic cell in order to track the label-free signals. No specific interaction is expected to be observed on the “reference” spots that were blocked with BSA.

Monoclonal anti-human Ang2 antibody (a-Ang2⁽¹⁾, P.N.MAB0983 from R&D Systems) was diluted to 20 µg/ml in the running buffer (D-PBS 1x containing 0.1% wt BSA) and injected in the fluidic channel. After such immobilization step and rinsing with buffer the biochip was ready for Ang2 detection. Therefore injection of a 50 ng/ml Ang2 solution in the buffer (recombinant human Ang2, P.N.623-AN from R&D Systems) was performed. A further specific polyclonal detection human Ang2 biotinylated antibody (a-Ang2⁽²⁾, P.N. BAF623 from R&D Systems) with a concentration of 2 µg/ml was then injected in order to recognize the surface bound antigen. Biotinylation enables one to introduce fluorescent labels in a last step by injecting a solution of 10 µg/ml NeutrAvidin650 (NeutrAvidin, DyLight 650 conjugated from Thermo Scientific). Thus, fluorescence emission will indicate the presence of antigen at the biochip surface. In-between all steps, the sensor surface was typically washed with the buffer to remove any proteins or antibodies that are non-specifically bound. BSA was not present in the buffer before and after NeutrAvidin650 injection.

5. RESULTS

The label-free tracking of the resonance position vs. time is shown in Figure 5(a). In order to correct for drifts of the resonance position due to temperature fluctuations, bulk refractive index changes and laser wavelength instability, the reference measurement has been subtracted from the signal obtained on the Protein G-coated spot. As Figure 5(b) illustrates, signal drifts can be removed and clear binding signals are obtained. The fast oscillations of the signal are introduced by forward and backward pumping of the protein solutions across the sensor surface during interaction.

Following an initial buffer step, the capture antibody has been injected at about $t \sim 2$ min. The temporal behavior can be well associated with a binding curve. Rinsing with buffer around $t \sim 20$ min yields a decreasing signal that is associated to a dissociation of excess unbound antibodies from the surface. Injecting the analyte solution containing 50 ng/ml Ang2 at $t \sim 23$ min yields a clear positive slope of the difference signal, indicating a net increase of mass density at the measurement surface due to the specific detection of Ang2 via the capture antibody. This conclusion is further supported by the binding like behavior when injecting the second a-Ang2⁽²⁾ antibody to detect the analyte molecule (Ang2). Therefore, a successful label-free detection of 50 ng/ml Ang2 is concluded.

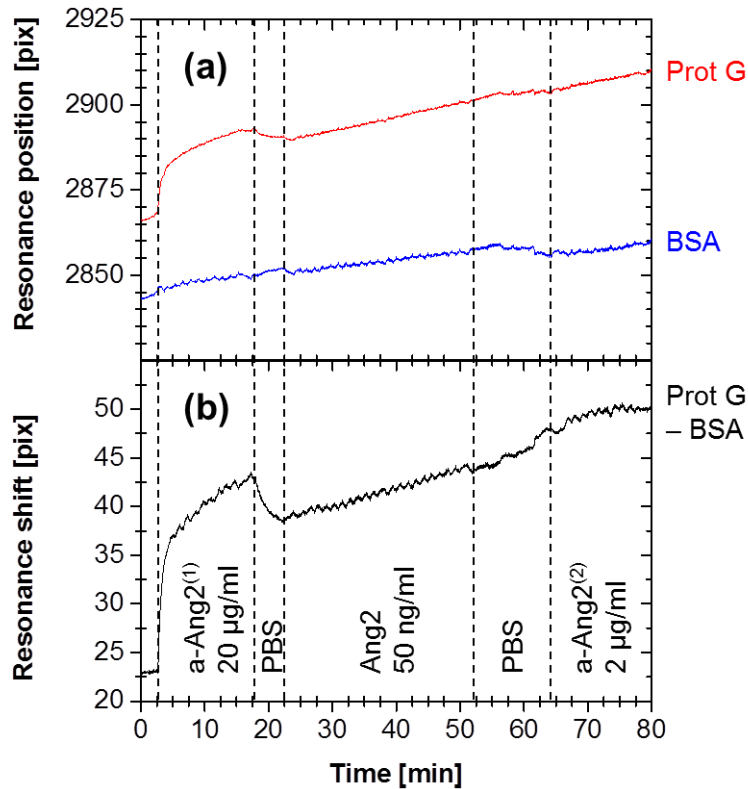


Figure 5. Label free assay detecting Ang2: (a) Raw data of BSW resonance position vs. time for one measurement (Prot G) and one reference (BSA) spot; the reference signal has been shifted for proper scaling of the diagram. (b) Difference signal of the two curves shown in (a).

As described in section 4, the second antibody (last binding step in Figure 5) can be labelled that allows the comparison of the fluorescence intensities obtained from the two different surfaces. Therefore, the fluorescence has been analyzed prior and after such labelling of a-Ang2⁽²⁾ with fluorescent label NeutrAvidin650. The difference of the angular fluorescence intensities before and after labelling is shown in Figure 6 for the measurement and the reference surfaces. According to the fluorescence spectra the second antibody could be successfully detected on the Protein G-coated surface, while practically no fluorescence increase is obtained at the BSA-coated spots. This supports the conclusion drawn from the label free experiment.

The shape of the angular spectrum detected in Figure 6 agrees well with the prediction shown in Figure 3. Dye labels couple their excitation energy to both surface wave polarizations. Two peaks are observed in the emission angular spectrum. Due to the fact that the dispersion of the surface wave is known, such angular spectrum is a representation of the spectral emission. Note, that the wavelength – angle relation is not similar for both polarizations. Furthermore, it is in general non-linear (compare Figure 2). That's why the two arrows indicate the wavelength scale direction only, without showing a second axis.

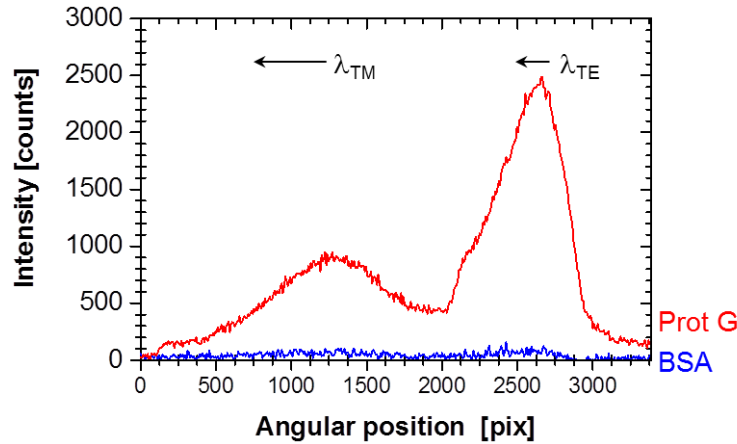


Figure 6. Fluorescence spectra corrected for background signal obtained after fluorescent labelling of the biotinylated secondary antibody with NeutrAvidin650 as described in section 4. The two peaks correspond to the different polarizations of the surface mode; the arrows indicate the wavelengths of emission associated with the angle of observation due to the surface wave dispersion.

6. CONCLUSIONS

The present work describes an approach based on BSW to combine label-free experiments with the features of detecting fluorescent labels. Low loss dielectric stacks have been prepared on injection molded chips in order to exploit narrow surface wave resonances. Furthermore, injection molded flow cells have been fabricated to seal the chip after preparation. All such technologies are available for large scale production thus making the chip approach a valid candidate for disposable biosensor application.

A sandwich assay that detects cancer biomarker Angiopoietin-2 has been successfully demonstrated via this approach. The tracking of the angular resonance position yields a label-free detection that allows to observe all binding steps of the sandwich assay. A concentration of 50 ng/ml Ang2 in PBS buffer has been analyzed as example. This result is supported by the clear difference of fluorescence intensities obtained on measurement and reference spots, indicating a potentially much lower limit of detection. As a whole, successful combination of label-free and fluorescence modes in one optical detection system is achieved.

In addition to the assay optimization and thorough testing of the limit of detection, the lateral resolution of the detection system should enable analyzing up to ~20 measurement spots on the sensor surface allowing multiple analyte detection. Several of these features of the present system are under investigation and will be reported in due course. Notably, the combination of spectral and wavelength resolution in fluorescence mode yields new parameters for read-out that opens up new possibilities for designing different assays.

ACKNOWLEDGMENT

This work has been funded by the European Commission through the project BILOBA (www.biloba-project.eu; Grant agreement 318035). The authors are grateful to P. Rivolo and E. Descrovi (Politecnico di Torino, Italy) and L. Napione

(Università di Torino, Italy) for initial discussions, as well as B. Höfer and R. Rosenberger (Fraunhofer IOF, Jena, Germany) for setting up the optical system.

REFERENCES

- [1] Homola, J., "Surface plasmon resonance sensors for detection of chemical and biological species," *Chem. Rev.* 108, 462-493 (2008)
- [2] Homola, J., Yee, S. S. and Gauglitz, G., "Surface plasmon resonance sensors: review," *Sens. Act. B* 54, 3-15 (1999)
- [3] Yeh, P., Yariv, A. and Hong, C.-S., "Electromagnetic propagation in periodic stratified media. I. General theory," *J. Opt. Soc. Am.* 67(4), 423-438 (1977)
- [4] Robertson, W. M. and May, M. S., "Surface electromagnetic wave excitation on one-dimensional photonic bandgap arrays," *Appl. Phys. Lett.* 74(13), 1800-1802 (1999)
- [5] Shinn, M. and Robertson, W. M., "Surface plasmon-like sensor based on surface electromagnetic waves in a photonic band-gap material," *Sens. Act. B* 105, 360-364 (2005)
- [6] Konopsky, V. N. and Alieva, E. V., "Photonic crystal surface wave for optical biosensors," *Anal. Chem.* 79(12), 4729-4735 (2007)
- [7] Sinibaldi, A., Danz, N., Descrovi, E., Munzert, P., Schulz, U., Sonntag, F., Dominici, L. and Michelotti, F., "Direct comparison of the performance of Bloch surface wave and surface plasmon polariton sensors," *Sens. Act. B* 174, 292-298 (2012)
- [8] Sinibaldi, A., Rizzo, R., Figliozzi, G., Descrovi, E., Danz, N., Munzert, P., Anopchenko, A. and Michelotti, F., "A full ellipsometric approach to optical sensing with Bloch surface waves on photonic crystals," *Opt. Expr.* 21(20), 23331-23344 (2013)
- [9] Rizzo, R., Danz, N., Michelotti, F., Maillart, E., Anopchenko, A. and Wächter, C., "Optimization of angularly resolved Bloch surface wave biosensors," *Opt. Expr.* 22(19), 23202-23214 (2014)
- [10] Ballarini, M., Frascella, F., Michelotti, F., Digregorio, G., Rivolo, P., Paeder, V., Musi, V., Giorgis, F. and Descrovi, E., "Bloch surface waves-controlled emission of organic dyes grafted on a one-dimensional photonic crystal," *Appl. Phys. Lett.* 99(4), 043302 (2011)
- [11] Sinibaldi, A., Fieramosca, A., Rizzo, R., Anopchenko, A., Danz, N., Munzert, P., Magistris, C., Barolo, C., and Michelotti, F., "Combining label-free and fluorescence operation of Bloch surface wave optical sensors," *Opt. Lett.* 39(10), 2947-2950 (2014)
- [12] Danz, N., Kick, A., Sonntag, F., Schmieder, S., Höfer, B., Klotzbach, U. and Mertig, M., "Surface plasmon resonance platform technology for multi-parameter analyses on polymer chips," *Eng. Life Sci.* 11(6) 566-572 (2011)
- [13] Holash, J., Wiegand, S. J. and Yancopoulos, G. D., "New model of tumor angiogenesis: dynamic balance between vessel regression and growth mediated by angiopoietins and VEGF," *Oncogene* 18, 5356-5362 (1999)
- [14] Ahmad, S. A., Liu, W., Jung, Y. D., Fan, F., Reinmuth, N., Bucana, C. D. and Ellis, L. M., "Differential expression of Angiopoietin-1 and Angiopoietin-2 in colon carcinoma," *Cancer* 92(5), 1138-1143 (2001)
- [15] Munzert, P., Schulz, U. and Kaiser, N., "Transparent thermoplastic polymers in plasma assisted coating processes," *Surf. Coat. Tech.* 174-175, 1048-1052 (2003)
- [16] Sinibaldi, A., Anopchenko, A., Rizzo, R., Danz, N., Munzert, P., Rivolo, P., Frascella, F., Ricciardi, S. and Michelotti, F., "Angularly resolved ellipsometric optical biosensing by means of Bloch surface waves," *Anal. Bioanal. Chem.*, published online DOI 10.1007/s00216-015-8591-8 (2015)
- [17] Danz, N., Waldhäusl, R., Bräuer, A. and Kowarschik, R., "Dipole lifetime in stratified media," *J. Opt. Soc. Am. B* 19(3), 412-419 (2002)
- [18] Flämmich, M., Frischeisen, J., Setz, D. S., Michaelis, D., Krummacher, B. C., Schmidt, T. D., Brütting, W. and Danz, N., "Oriented phosphorescent emitters boost OLED efficiency," *Org. Electron.* 12, 1663-1668 (2011)
- [19] see "DyLight® Fluorochrome conjugated secondary antibodies" under <http://www.abcam.com/index.html?pageconfig=resource&rid=12934>
- [20] Henseleit, A., Pohl, C., Bley, T. and Boschke, E., "Monitoring human serum albumin cell cultures using surface plasmon resonance (SPR) spectroscopy," *J. Sens. Sens. Syst.* 4, 77-83 (2015)
- [21] Chamas, A., Giersberg, M., Friedrich, K., Sonntag, F., Kunze, D., Uhlig, S., Simon, K., Baronian, K. and Kunze, G., "Purification and immunodetection of the complete recombinant HER-2[neu] receptor produced in yeast," *Protein Expression and Purification* 105, 61-70 (2015)